26th EPS Conf. on Contr. Fusion and Plasma Physics, Maastricht, 14 - 18 June 1999 ECA Vol.23J (1999) 1645 - 1648

L-H Transport Barrier Formation: Neoclassical Simulation and Comparison with Tokamak Experiments

J.A. Heikkinen(1), T.P. Kiviniemi(2), A.G. Peeters(3), T. Kurki-Suonio(2), and S.K. Sipilä(2)

(1) *VTT Energy, Euratom-TEKES Association, Finland*

(2) *Helsinki University of Technology, Euratom-TEKES Association, Finland*

(3) *Max-Planck-Institut für Plasmaphysik - EURATOM Association, Germany*

Abstract: Monte Carlo ion simulation of the plasma edge based on neoclassical radial current balance in a tokamak shows no spontaneous bifurcation of radial electric field E_r in contrast with earlier orbit loss models, but bifurcation and a solitary E_r generation by electrode polarization is seen. The parameter scaling of threshold temperature for strong turbulence shear suppression as obtained from MHD turbulence simulation agrees with the H-mode threshold scaling in ASDEX Upgrade.

Introduction: For the first time, the dynamics of the radial electric field E_r and its bifurcation are solved with a fully kinetic 5D neoclassical Monte Carlo simulation of the tokamak edge. L-H transition in experiments has been observed to occur spontaneously with sufficient external heating or, also in Ohmic plasmas, with electrode polarization. An important theory aiming to explain this transition is based on a multi-valued solutions of radial current [1]. The problem is difficult because the ion orbits can have a width comparable to the gradient lengths in the edge violating the standard neoclassical theory. A fraction of ions can escape over the separatrix and be lost on the wall or target plates, creating a nonambipolar flux, that drives E_r. The field itself can in turn influence the orbits through, e.g., squeezing. Collisions prevent completion of ion orbits and reduce the loss current, while the velocity loss cone is populated through collisions. The bulk ions are important since they carry the return current, which is generated through the viscous damping of the (non-vanishing) poloidal rotation, and cannot be separated from the loss current carriers. Finally, perpendicular viscosity can play a role for large flow gradients. This complex interplay among several mechanisms requires a self-consistent computation. Here, all these effects are included in evaluating E_r from the orbit following Monte Carlo code ASCOT [2] applied for the ASDEX Upgrade and TEXTOR.

Model: In ASCOT, the ion ensemble is initially distributed according to the assumed background n and T with Maxwellian energy distribution. Each ion is followed along its guiding-centre orbit determined by the $\vec{E} \times \vec{B}$, gradient and curvature drifts, momentum and energy conserving collisions, polarization and viscosity drifts. The radial electric field $E_r(\rho) = -(d\Phi(\rho)/d\rho)\langle d\rho/dr\rangle$ on the magnetic surface with the coordinate ρ is evaluated from $\partial E_r/\partial t = -\Omega B_t \langle v_r\rangle_{NC}$, where $\Omega = ZeB/m_i$ and B_t are taken at the magnetic axis, and $\langle v_r\rangle_{NC}$ is the flux surface (and ensemble) average of the ion radial velocity at the radius ρ as calculated from ion motion excluding the polarization drift.

The field is solved with the neoclassical ambipolar $E_r = (k_B T/Ze)[(dn/d\rho)/n + \gamma(dT/d\rho)/T]\langle d\rho/dr\rangle$ as an initial condition. The outer boundary for the E_r evaluation is at the separatrix $\rho = \rho_s$. For $\rho > \rho_s$, $E_r(\rho_s) = 0$ is adopted. The ions are initialized within $\rho_L < \rho < \rho_s$, and those hitting the divertor plates or walls outside $\rho > \rho_s$ are reinitialized at the separatrix uniformly in pitch and poloidal angle with the local Maxwellian velocity distribution at $\rho = \rho_s$. This simulates well the replacement of the lost charge being more uniform in phase space than the loss process. As the ambipolar transport does not affect the current, it is not considered. Perpendicular Braginskii viscosity drift $\langle v_r \rangle_v = -(\eta/B^2)\partial^2 E_r/\partial\rho^2 \langle d\rho/dr \rangle^2$ is added to $\langle v_r \rangle_{NC}$ in the polarization equation.

Results: Steady-state is found by continuing the calculation for some ms. Alternatively, steady-state with $dE_r/dt = 0$ has been found by directly iterating the E_r profile until the given n profile is found. Both methods have resulted with the same steady-state independent of the initial E_r indicating that the final state is stable and unique.

In the ASDEX Upgrade, the minor radius is $a = 0.5$ m, $R = 1.65$ m, elongation 1.6, $I = 1$ MA, and $B_t = -2.5$ T. Corresponding to the shot #8044 for a deuterium plasma, a separatrix density 1.2×10^{19} m^{-3} and temperature 120 eV with about 1.9 times larger values at $r = a - 2$ cm are adopted for reference. Fig. 1 shows the steady-state profiles of $-d\Phi/d\rho$ in the region $0.96 < \rho < 1$ ($\rho_s = 1$) for various temperatures. E_r on the outboard equator is found from $d\rho/dr = 2$ m^{-1}. E_r is at an ambipolar level for $|r - a| > 1 - 2$ cm with the Mach number $M = |E_r/B_p v_T|$ of the rotation less than one. The decrease of E_r within $|r-a| < 1$ cm is larger typically by an order of magnitude than the $1 - 2$ kV/m decrease of the ambipolar value. Figure shows that the BDT criterion [3] can be well satisfied in a wide enough region, if T is large. Consistent with ASDEX Upgrade experiments, deuterium gives higher shear (i.e., lower H-mode threshold) than hydrogen. Simulation gives for tritium the highest shear and helium the lowest. With n and B_t the shear increases only weakly. The E_r profiles in Fig. 1 resemble the measured E_r profiles at the transition in DIII-D [4] for the width or depth of the well. Also, the profile is robust to the plasma parameters, and the shear rate is unsensitive to the divertor configuration, as checked by modifying the position and number of the divertor plates. Effects of B_t ripple ion losses were found weak, too. According to the simulations, the obtained stationary states are the only solutions, and no bifurcation is found, even when $\nu_i^\star$ drops below one, in contrast to earlier orbit loss (OL) theories [1].

As $\langle j_r \rangle = 0$, toroidal rotation was irrelevant in E_r dynamics. Simulations were also performed for the biased experiments [5] where E_r is imposed externally by a polarization electrode in the edge and $\langle j_r \rangle \neq 0$ in the plasma. Here, the electrode current I_E and E_r profile were solved by keeping a given voltage between the electrode tip and limiter. Like in TEXTOR experiments [5], bifurcation in I_E at a transition voltage U_{cr} was found. E_r profile bifurcated from a uniform shape to a solitary structure. Fig.2 shows the I_E-voltage curve and the soliton evolution for a 450 V voltage with the TEXTOR parameters [5] assuming no neutral damping. This gives the first numerical evidence of the soliton solutions suggested recently in [6]. The OL current was here weak. The solitons appeared within ~ 2 cm from a with position, width, and height dependent on η, viscosity, and neutral damping profile. Also U_{cr} and I_E were found to be sensitive to neutral damping ($U_{cr} \approx 450$ V was simulated with a 7 % neutral fraction with 2 cm exponential decay length). The neoclassical viscosity model was further confirmed by simulations of poloidal rotation relaxation rate with fixed E_r in the absence of OL [7]. As bifurcation is found with external current, but not spontaneously, self-consistency in treating radial current carriers appears crucial in proper description of E_r dynamics.

Requiring $(1/L)\int_{a-L}^{a} H(\langle dE_r/dr \rangle/B - 5 \times 10^5)dr > 0.7$ with $L = 1$ cm that the shear exceeds a value 5×10^5 s^{-1} at least within 0.7 cm just inside the separatrix, the critical temperature T_{cr} for transition from low to high shear and its parameter dependence on n, B_t, and I have been estimated. H denotes the Heaviside function. In ASDEX Upgrade experiments, the temperature for the onset of the H-mode was found to scale as $S(n, B_t, I) = 145 n^{-0.3}|B_t|^{0.8} I^{0.5}$ eV [8]. Here, n and T have been evaluated at $r = a - 2$ cm,

T is expressed in eV, n in 10^{19} m^{-3}, B_t in Teslas, and I in Mega-amperes. Fig. 3 shows the shear rate from ASCOT for various T and the function S with deuterium. A close agreement is found between the simulation and experiment. The parameters were varied in the range $B_t = -1.1 - (-5.0)$ T, $I = 0.6 - 1.5$ MA, $n = 0.6 - 12 \times 10^{19}$ m^{-3}, and $T = 30 - 400$ eV, broader than in the experiments. Shear dependence on n and T was found to be stronger in the lower n and T data range, respectively. With the threshold shear 5×10^5 s^{-1}, one obtains $T_{cr} = 126n^{-0.06}|B_t|^{0.76}I^{0.25}$ eV with ±0.25 error in exponents.

To show that the OL flow suppresses turbulence near T_{cr}, MHD turbulence with the simulated $\vec{E}\times\vec{B}$ flow was resolved. As a paradigm for self-organized tokamak plasma edge turbulence, resistive drift wave equations [9] for the nonlinearly unstable vorticity, density, temperature, and parallel electron velocity fluctuations were adopted, and were complemented with $\partial v_E/\partial t = \sum_{m=-M}^{M} imk_0(\Phi_{-m}\partial^2\Phi_m/\partial x^2)/B_0^2 + \nu[v(x,t) - v_E]$ describing the evolution of the average poloidal $\vec{E}\times\vec{B}$ velocity $v_E = \hat{z}\times\nabla\Phi_0/B_0 = (\partial\Phi_0/\partial x)\hat{y}/B_0$ in the presence of the electrostatic potential $\Phi = \sum_{m=-M}^{M}\Phi_m(x)\exp(imk_0y)$ and OL driven poloidal $\vec{E}\times\vec{B}$ flow $v(x,t)$. Here, a sheared two-dimensional slab with x and y corresponding to the radial and poloidal directions, respectively, was adopted with $L_y = 2\pi/k_0$ and $2L_x$ the lengths of the slab in the y and x directions. The first term on the above equation is the turbulent Reynolds stress and the second term with $\nu = qv_T/R$ models the viscosity. Single-helicity turbulence resonant at $x = 0$ and local magnetic shear $B = B_0(1 + x/L_s)$ with background gradients $dn/dx = -n_0/L_n$ and $dT/dx = -T_0/L_T$ were considered. Using our reference parameters, and $T_0 = 100$ eV, $n_0 = 4\times10^{19}$ m^{-3}, $L_n = L_T = 0.02$ m, $L_s = 2$ m, $L_y = 0.02\times\pi$ m, and $L_x = 0.015$ m, turbulence was followed for various shears $V' = dv/dx$ at $x = 0$ with nonlinearly unstable initial amplitudes of Φ_m. Fig. 4 shows the evolution of the kinetic energy $E_k = m\int_A|\nabla\hat{\Phi}/B_0|^2 da/2L_y$ in units of $mk_0^{-2}\omega_\star^2 r_L/2$ for $V' = 0, 3, 6$, and 9×10^5 s^{-1}. Here, $\omega_\star = k_0T_0/eB_0L_n$ is the drift wave angular frequency, r_L is the ion Larmor radius, $\hat{\Phi} = \Phi - \Phi_0$, and $\int_A$ denotes surface integral over the slab. $2M + 1 = 121$ modes with 151 grid points in x were used. A nonlinearly saturated turbulence with a strongly suppressed level for largest V' is found. Suppression grows gradually with V' and becomes significant for $V' \sim 5\times10^5$ s^{-1}. Similar threshold was also found with the pressure-gradient driven turbulence. Turbulence suppression and perturbations in v_E by the Reynolds stress were weak and always dominated by the OL driven flow near the threshold in Fig. 3.

Conclusions: Some experiments [10] see a neoclassical ambipolar E_r just before the transition and a fast suppression of turbulence at the transition on a time scale much shorter than changes in background T. To reconcile our findings with them, a mechanism restraining OL driven rotation in (low shear) L-mode and allowing it in (high shear) H-mode is required. Any deviation of our T_{cr} scaling from experiment may be explained by such an additional mechanism, but as shown here for ASDEX Upgrade, such corrections may not be strong with major scaling arising from the OL driven shear.

References:

[1] K.C. Shaing and E.C. Crume, Jr., Phys. Rev. Lett. **63**, 2369 (1989)
[2] J.A. Heikkinen and S.K. Sipilä, Phys. Plasmas **2** (1995) 3724.
[3] H. Biglari, P.H. Diamond, and P.W. Terry, Phys. Fluids **B2**, 1 (1990).
[4] P. Gohil, K.H. Burrell, and T.N. Carlstrom, Nuclear Fusion **38**, 93 (1998).
[5] R.R. Weynants *et al.*, Nucl. Fusion **32**, 837 (1992)
[6] K. Itoh *et al.*, Phys. Plasmas **5**, 4121 (1998).
[7] T. Kiviniemi *et al*, submitted to Nuclear Fusion, 1999.

[8] W. Suttrop *et al*, Plasma Phys. Contr. Fusion **39**, 2051 (1997)
[9] B.D. Scott, Phys. Fluids **B4**, 2468 (1992).
[10] R.A. Moyer *et al*, Phys. Plasmas **2**, 2397 (1995).

Fig. 1

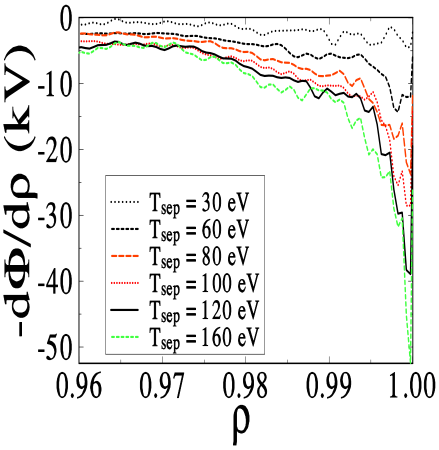

Fig. 2

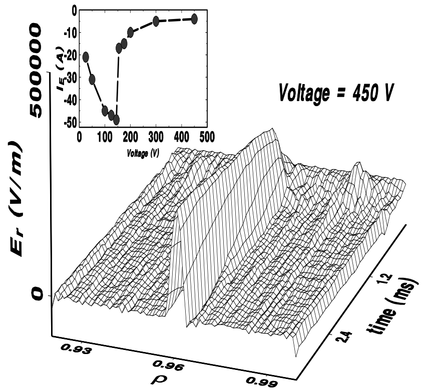

Fig. 3

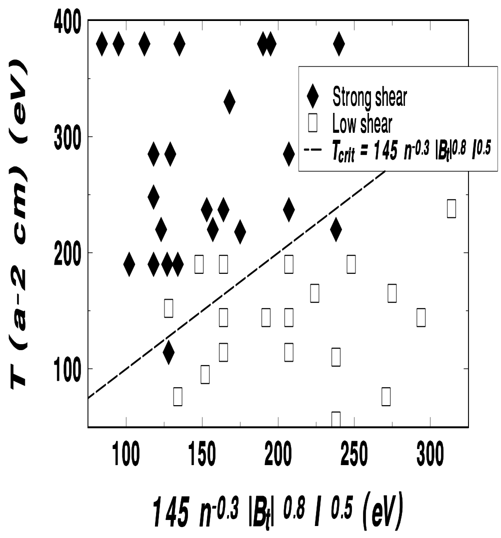

Fig. 4

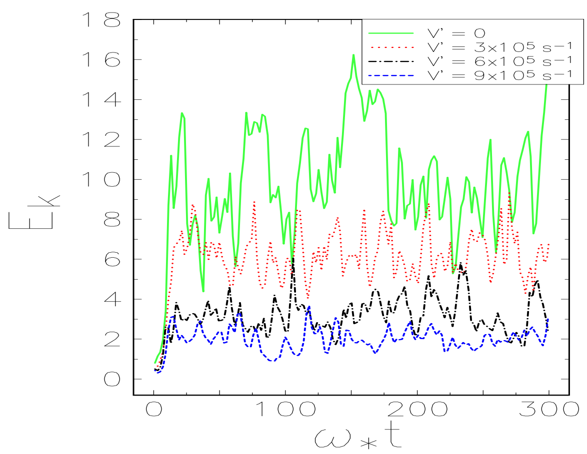

Fig. 1. $-d\Phi/d\rho$ *as a function of radius for various* T.
Fig. 2. E_r *as a function of radius and time for* 450 *V voltage as simulated for the TEXTOR polarization experiments starting with a uniform* E_r *radial profile.* I_E-*voltage curve is shown in the insert showing a transition at* $U_{cr} \sim 145$ *V.* $n = 2 \times 10^{18}$ m^{-3} *and* $T = 40$ *eV at* $r = a$. $I = 250$ *kA,* $B_T = 2.35$ *T,* $a = 0.46$ *m, and* $R = 1.75$ *m. Electrode tip - limiter distance is 4 cm.*
Fig. 3. Shear values of the $E_r \times B$ *flow as a function of the parameter* $S = 145n^{-0.3}|B_t|^{0.8}I^{0.5}$ *and temperature.*
Fig. 4. Kinetic energy E_k *in potential fluctuations (in arbitrary units) with various shears* V'.